

Pipeline Monitoring and Sensor Energy Analysis in Concessional Fog Wide Area Networks (CF-WAN)

¹F. N. Ugwoke

Dept. of Computer Science, Michael
Okpara University of Agriculture,
Umudike, Abia State, Nigeria
ndidi.ugwoke@gmail.com

²K. C. Okafor

Dept. of Mechatronics Engineering,
Federal University of Technology,
Owerri-Imo State, Nigeria
kennedy.okafor@futo.edu.ng

Abstract— *In this paper, the application of concessional Fog driven Wide Area Network (CF-WAN) with low powered edge sensor nodes is deployed in Pipeline flow monitoring (PFM) design. Energy demand assumption in Fog-WAN is used reduce cost savings in battery powered nodes. CF-WAN using Internet of things (IoT) energy integration is a novel contribution introduced. Mathematical characterization for various differential requirements in flow movements are discussed. Structural monitoring hierarchy (SMH) is formulated to meet the diverse service delivery concerns in Cloud queried pipeline-networks. Design considerations such as pipeline energy models, fluid pressures losses, fluid flow and location modelling are presented. Fog-WAN battery model for sustainable transceiver energy consumption model is investigated in the context of node deployment architecture. Energy consumption map of the transceiver edge-Fog WSN node battery model is developed. Metrics such as depth of charge (DoC), battery's state of charge (SoC), load current, load voltage, among others are analyzed. Validation use case simulation for characterized pipeline designs, flow equations, and pipeline detection parameters (event location) are presented. The results shows satisfactory proof of concept as well as reliable energy dissipation pattern for the pipeline traffic upload into the Cloud analytics dashboard.*

Keywords—*Internet of Things, Energy Models, Fluid dynamics, WAN, Pipeline designs, QoS.*

I. INTRODUCTION

Most fluid based natural resources are transported using flow-based technologies. With IoT based transceiver interfaces, real time data traffic can be aggregated for further analysis. The use of IoT-based WAN offers not only reliable monitoring, but appears very economical for distributed complex pipeline systems. A major application is found in damage detection process (DDP) known as structural health monitoring (SHM) [1]. This refers to the use of damage detection involving an array of sensors that are distributed uniformly to make periodic observations especially in dynamic response of the system. SHM has been employed in routine monitoring of buildings for safety (environmental monitoring) and cost reduction purposes [2]. In these systems, monitoring of parameters such as temperature, humidity, acceleration, tensile and compressive stresses and structural degradations are considered. In most cases, non-invasive approach is leveraged to deploy the sensors at endpoints. Legacy pipeline monitoring systems have various elements including the main body of the individual pipe segments, flanged and welded joints, valves, fittings, and

pumping stations. When pipeline systems are connected via IoT into the Cloud, real time monitoring will be affected by the structural integrity of the pipeline infrastructural segments involving flanged joints between the segments. Besides, with several vulnerabilities involving cyber-physical systems, energy sources must be protected within the context of IP flow network monitoring [3]. With the devastating issues of fluid flow management especially leakage detection, pipeline monitoring efforts has been intensified to minimize and eradicate wastes [4].

The use of IoT in SHM applications including smart grid, homes, cities, transport, etc, has changed the concept of infrastructural connectivity while allowing for massive sharing of data for insights managements and decision analysis. Pipeline sensors in context can actuate light, heat, pressure while using an energy conservation scheme to optimize its limited computation resources. With IoT clusters, monitoring of critical infrastructure including human activity can find useful applications in environmental, and control of production processes [4]. Most works have not explored CF-WAN Cloud transceiver system (WCTS) for sensor deployment, replacement in cases of natural fluid flow propulsions.

The main focus of this paper is to re-engineer pipeline monitoring using CF-WAN architecture. Essentially, fluid flow such as water, oil, gases as these play crucial roles in human existence. Large scale pipeline infrastructures needs to be setup to facilitate efficient transportation from the edge-to-edge while allowing for remote monitoring. To deploy a contextual use case, the SHM having pipeline arrays will be embedded with sensors at various points. The IoT nodes tracks structural integrity of the pipelines while maintaining energy conservation.

This research will implement a simulation proof of concept after deriving various sets of mathematical models for deployment pipeline design with the flow modes. Remote virtual Cloud endpoint will be used to demonstrate the status of edge pipeline for CF-WAN. For battery life preservation of the IoT nodes, the transceiver battery process model for parametric evaluations of the energy lifespan is shown. The pipeline equations, energy equations, localization and leakage detection algorithms, and flow continuity vis-à-vis a linear pipeline structure will be discussed. This will address the concerns of PFM using Fog-WAN driven by the IoT edge

layer. The rest of this paper is organized as follows. Section II discussed the related works in pipeline flow models, and research gaps. Section III focused on the methods and procedures applied in SHM system. Section IV provides the governance model for pipeline fluid flow energy system. Section V discussed CF-WAN IoT WSN. System validations is provided in Section VI while conclusion is presented in Section VII

II. RELATED WORKS

This Section defines Concessional Fog Wide Area Networks (CF-WAN) as an extended edge computing network meant for hierarchical connectivity into the Cloud. This uses the Fog layers for latency minimization [5], [6]. Various efforts on Fog-WAN discussed how generated volumetric or datacentric streams are used to make decisions [7-10].

Both the control and data planes of the CF-WAN processes services as the edge while allowing proximity to end-points. Hence, both the computational resources and QoS are easily handled. Cathodic protection was applied in monitoring of oil and natural gas pipelines using linear wireless sensor networks in [11]. Fiber Bragg Grating scheme was discussed for handling pipeline based landslide monitoring designs leveraging GPRS module [12]. High reliability and flexible network distribution characterizes field monitoring of pipelines buried in the context of environmental disasters.

The work [13] discussed low cost-low energy monitoring model for underground pipelines. Also, adaptive duty-cycle MAC protocol was introduced while considering Wake-on-radio called WoR-MAC. In [14], pipeline distributed parametric system was investigated using an infinite dimension for observability, and controllability analysis in the pipeline systems. In [15], [16], leak diagnosis scheme for maintaining the integrity and efficiency of pipelines was discussed in real-world context using low-cost XBee technology.

In [17], pipeline acoustic detection for submarine pipelines was discussed for monitoring buried submarine pipelines. Multi-sensor surveying system was introduced for integrating sub-bottom profiler (SBP) and the Shipborne Over- and Under-Water Integrated Mobile Mapping System (SiOUMMS) on the same ship while doing various pipeline analysis. Real-Time leakage detection has been investigated in [18-24].

The works [25-33] focused on pipeline monitoring, diagnostics of underground pipelines, corrosion monitoring system, tracking of buried oil and gas pipelines and geotagging, sparse spatiotemporal feature learning for pipeline anomaly detection, data pre-processing algorithm and fault recognition technology for pipeline systems.

The major gaps in existing works include: absence of CF-WAN elements include: transceiver power, transceiver robustness, transceiver communication, transceiver CPU computation, transceiver time synchronization for edge to Cloud transactions. The works have not reported efforts in wireless transceiver battery cell with critical mathematical models.

III. METHODOLOGY

A. Architectural Structure

This work developed a system architecture that supports edge-to-Fog and Fog-to-Cloud pipeline monitoring. Using invasive MKR 1000 embedded system (IoT module), the cyber-physical network topology is designed for the pipeline architecture. This is done using layered organization as shown in Figure 1 while Figure 2 shows the battery module.

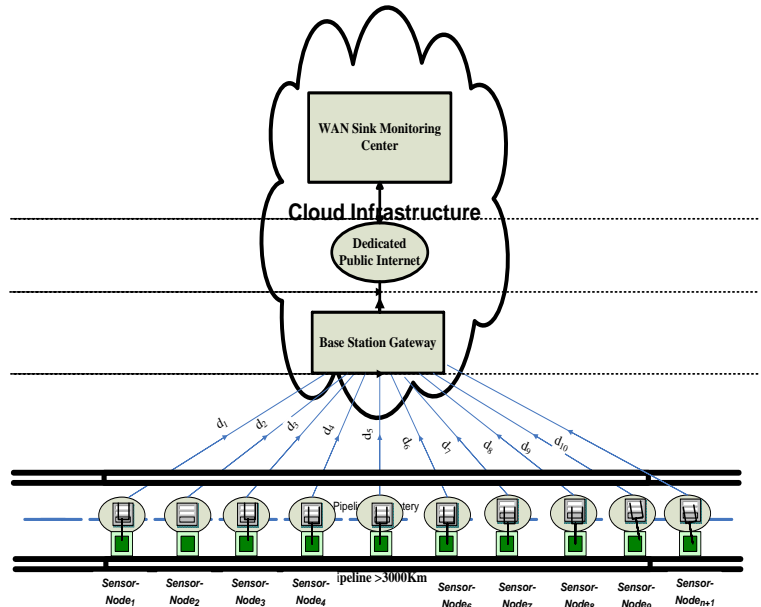


Fig. 1. CF-WAN Pipeline infrastructure.

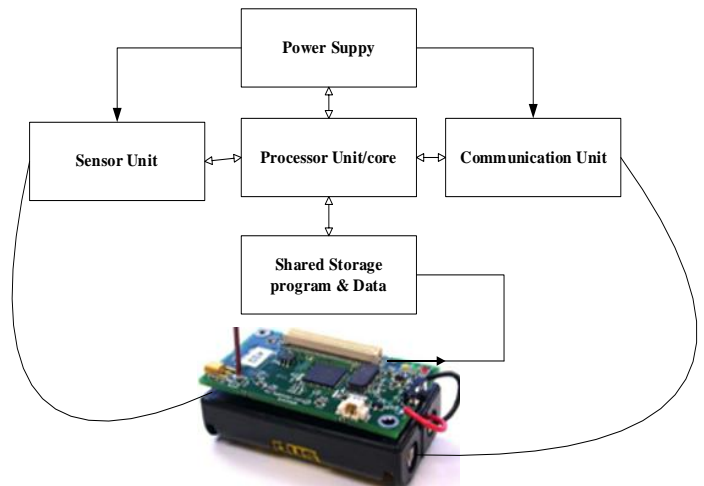


Fig. 2. IoT CF-WAN node internal architecture.

The CF-WAN uses a robust and resilient communication backbone to achieve seamless data transmissions. This comprises the edge-access layer, the Fog base station and the gateway internet aggregation layer.

At the edge layer having the deployed pipelines, the IoT nodes are physically attached to the pipeline layouts (i.e., IoT nodes n to $N+1$). This communicates with the distances d_1 to d_{n+1} to the base station gateway before relaying the event data to the sink. The IoT nodes satisfy the requirements showed in Figure 2. The IoT nodes (MK1000) are attached non-invasively considering the outdoor/indoor event sensing and

communication. From Figure 2, the edge cluster head deployment in a multi-hop communication domain is much closer the Cloud gateway which carried out monitoring operation. The energy management algorithms handles node energy consumption in the multi-hop communication mode.

The major merits of the layered model include: satisfactory event location sensing and tracking, high speed, reduced overhead with very little management/maintenance concerns. Also, it offers lower energy consumption. The identified architectural attributes in Figure 1 include: traffic concurrency, architectural flexibility, synchronization, RF decoupling and low latency. At transmission mode, fixed power is used while reducing the energy consumption of the IoT nodes. With optimal power management (OPM), a decoupling scheme for transmission rate transmission is achieved. The assigned battery model for interacting with the radio was deployed based on OPM.

B. CF-WAN Pipeline SHM

Considering Figure1, the SHM based edge layered pipeline system (CF-WAN) supports sensor based integration for monitoring vandalization, leakage and other issues such as IoT pipeline deployment design, fluid-flow dynamics, pipeline losses due to friction, flow energy equation, IoT sensor energy equations and models, and event location model for vandalization. The model addressed possible pipeline failures such as link failures and a multi-tenanted incremental upgrade scheme for fluid monitoring. For efficiency in CF-WAN integration, an interconnection of remote WAN server clusters with Fog gateway provides higher network capacity for low latency packet delivery and congestion free network.

At the edge layer, the pipeline deployment is used for transporting fluids from location A to location N. In context, the oil and gas industry uses pipeline that can resist pressures more than 4N/nm² and temperature greater than 440°C. Hence, an introduction of pipeline network for fluid flow is re-engineered. The pipeline design considered the internal diameter and its wall thickness t , pipeline stress design and joints for circular or oval flanged pipeline structures.

C. Design Model For WSN Pipeline Deployment

Figure 3 shows a use case pipeline deployment layout carrying fluid x with a density dx . The design of the pipeline involves the determination of the inside diameter of the pipe D and its wall thickness t for the fluid flow. IoT based wireless sensors nodes are placed invasively in the design. This is to allow for direct measurement of all control and process variables.

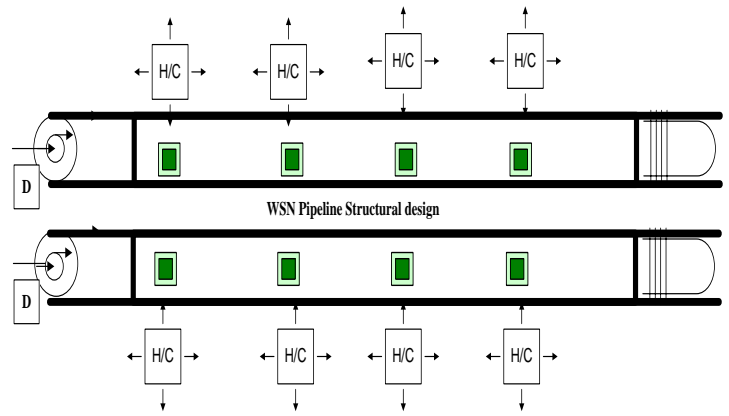


Fig. 3. CF-WAN pipeline layout.

D. Inside Diameter Piepline Equations

This depends on the quantity of the oil fluid to be delivered, as such, Let,

A represent the cross sectional Area of the pipe

D represent the diameter of the pipe

V represent the velocity of pipeline fluid per minute

Q represent Quantity of fluid carried per minute

But the Quantity Q of fluid flowing per minute

is given by:

$$Q = A * V = \frac{\pi}{4} * D^2 * V \quad (1)$$

Solving for D in Equ.1 gives

$$D = \sqrt{\frac{4 * Q}{\pi * V}} = 1.13 \sqrt{\frac{Q}{V}} \quad (2)$$

E. Pipeline Wall Thickness t

From Figure 3, t is considered next in order to withstand the internal fluid pressure p in the thin or thick cylindrical pipeline.

Essentially, the thin cylindrical equation will be applied when:

- i. Stress across the pipeline section is uniform.
- ii. The internal diameter of the pipeline section D is $>20t$ i.e. $D/t > 20$.
- iii. The allowable stress σ_t is more than six times the pressure inside the pipe P i.e. $\sigma_t > 6P$.

According to the thin cylindrical equ, wall thickness t of the pipeline is given by Equ. (3)

$$t = \frac{P.D}{2Q_t} = \frac{P.D}{2Q_t \eta_t} + C \quad (3)$$

Where, η_t is the Efficiency of longitudinal joint and C is the Weishack constant

F. WSN Pipeline Stress Design Model

Consider a cylindrical shell of a pressure vessel carrying oil fluid which was subjected to a high internal fluid pressure p , the wall of the cylinder must be made extremely thick t .

Assuming that the tensile stresses are uniformly distributed over the section of the walls, let,

r_0 represent outer radius of the cylindrical shell
 r_i represent inner radius of the cylindrical shell
 t represent thickness of the cylindrical shell = $r_0 - r_i$
 p represents intensity of internal pressure
 μ represent poisson's ratio
 σ_t represents tangential stress
 σ_r represents radial stress

Using lame's law which states that assuming that the longitudinal fiber of the cylindrical shell are strained, the tangential stress at any radius x is given by

$$\sigma_t = \frac{p_i(r_i)^2 - p_0(r_0)^2}{(r_0)^2 - (r_i)^2} + \frac{(r_i)^2(r_0)^2}{x^2} \left[\frac{p_i - p_0}{(r_0)^2 - (r_i)^2} \right] \tag{4}$$

Now, radial stress at any radius x is given by

$$\sigma_r = \frac{p_i(r_i)^2 - p_0(r_0)^2}{(r_0)^2 - (r_i)^2} - \frac{(r_i)^2(r_0)^2}{x^2} \left[\frac{p_i - p_0}{(r_0)^2 - (r_i)^2} \right] \tag{5}$$

Considering the internal pressure only $P_i = P$ and let external pressure, $P_0 = 0$,

From Equ 3, the tangential stress at any radius x is given by.

$$\sigma_t = \frac{p_i(r_i)^2}{(r_0)^2 - (r_i)^2} \left[1 + \frac{(r_0)^2}{x^2} \right] \tag{6}$$

$$\sigma_r = \frac{p_i(r_i)^2}{(r_0)^2 - (r_i)^2} \left[1 - \frac{(r_0)^2}{x^2} \right] \tag{7}$$

From Equ. (6) and (7), the tangential stress is a tensile stress whereas the radial stress is a compressive stress.

Again, the tangential stress is Maximum at the inner surface of the pipeline, i.e. $x = r_i$ and it is minimum at the outer surface of the shell i.e. $x = r_0$

By taking the value of $x = r_i$ and $x = r_0$ in Equ. (6) and (7), the Maximum tangential stress at the inner surface of the pipeline is given by,

$$\sigma_{(t_{Max})} = \frac{p[(r_0)^2 + (r_i)^2]}{(r_0)^2 - (r_i)^2} \tag{8}$$

While the minimum tangential stress at the outer surface of the shell is given by,

$$\sigma_{(t_{Min})} = \frac{2P[(r_i)^2]}{(r_0)^2 - (r_i)^2} \tag{9}$$

$\sigma_{(t_{Max})} = -p$ (Compressive) and at $\sigma_{(t_{Min})} = 0$

Therefore, Equ. (8) and (9) becomes the major maximum and minimum stress equation for the WAN WSN pipeline design.

G. WSN Pipeline Joint Design Model

In pipeline monitoring, for a circular flanged pipeline joint, it is assumed that the fluid pressure acts in between the flanges and tends to separate them with a pressure existing at the point of leaking. However, bolts are required to take up tensile stress in order to keep the flanges together. Now, let, the effective diameter on which the fluid pressure acts just at

the point of leaking be the diameter of a circle touching the bolt holes.

Let this diameter be D_l . If d_l is the diameter of bolt hold and D_p is the pitch circle diameter, then,

$$D_l = D_p - d_l \tag{10}$$

Hence, from Equ. (10), force trying to separate the two flanges is given by,

$$F = \frac{\pi}{4} * (D_l)^2 * P \tag{11}$$

Now, to compute the resistance of the tearing of bolts, Let n = Number of bolts,

d_c = Core diameter of the bolts

$\sigma_{(t)}$ = permissible stress for the material of the bolts
Hence, resistance R , is then given by,

$$F = \frac{\pi}{4} * (d_c)^2 * \sigma_{(t)} * n \tag{12}$$

IV. GOVERNANCE MODEL

A. WSN Pipeline Fluid Flow Energy System

Understanding the dynamics of the pipeline fluid flows before discussing the event location tracking is the concern addressed in this section. In a real pipeline deployment, fluid flows has equivalent mathematical models. Now, fluids possess viscosity, hence loses energy due to friction. These fluid properties interact with one another as well as with the pipe walls. The emphasis is on the monitoring of the fluid flow leakages and location using IoT WSN transceiver CF-WAN Cloud. Hence, let's consider the mathematical representations of these fluid flow dynamics.

Let, the shear stress induced in a fluid flowing near a boundary be given by Newton's law of viscosity, viz:

Shear stress τ in a fluid is proportional to the velocity gradient- i.e the rate of change of velocity across the fluid path, hence,

$$\text{Shear Stress } \tau \propto \frac{du}{dy} \tag{13}$$

$$\tau = \mu \frac{du}{dy} \tag{14}$$

Where μ is the coefficient of viscosity,
Flows in Pipelines can be classified into laminar or turbulent flow, but a non-dimensional number, called the Reynolds number, Re is used to determine which type of flow that occurs. This is given by

$$Re = \rho \frac{U_d}{\mu} \tag{15}$$

Generally, in a pipeline,
Laminar Flow: $Re < 2000$
Transitional flow: $2000 < Re < 4000$
Turbulent Flow: $Re > 4000$ (16)

By determining the flow type from Equ.1.3, this governs how the amount of energy lost to friction relates to the viscosity of the flow. Hence, how much energy must be used to move the fluid.

B. Pipeline Pressure Loss

As a result of Friction there are possible pressure losses.

Consider a cylindrical element of incompressible fluid flowing in the pipe as shown in Figure 4. The pressure of the upstream end L_1 is P and the at the downstream end L_2 , the pressure has fallen by

$$P = \Delta p \text{ to } (P - \Delta p) \quad (17)$$

The driving force due to pressure ($F = \text{Pressure} * \text{Area}$) can be represented by

Driving pressure,

$Dp = \text{Pressure Force at } L_1 - \text{pressure force at } L_2$, given by

$$PA - (P - \Delta p)A = \Delta p A = \Delta p \frac{\pi d^2}{4} \quad (18)$$

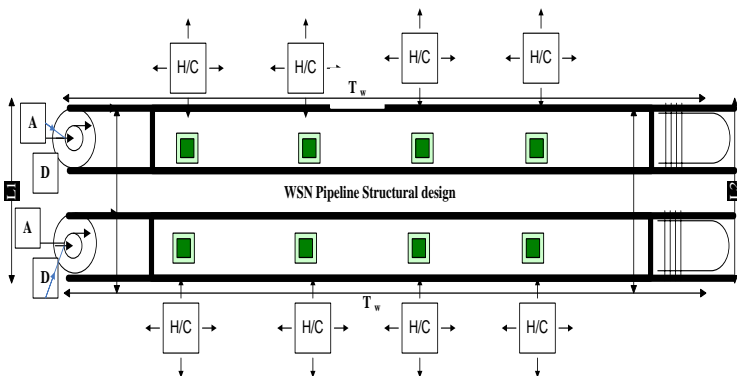


Fig. 4. Element of fluid in a Pipeline.

The retarding force due to the shear stress by the walls is given by,

$Fr = \text{Shear Stress} * \text{Area over which it acts}$

$Fr = \tau_w * \text{Area of Pipewall}$

$$Fr = \tau_w * \pi d L \quad (19)$$

As the flow gets to equilibrium, the driving force = retarding force, i.e., Equ 18 = Equ 19

$$\Rightarrow \Delta p \frac{\pi d^2}{4} = \tau_w * \pi d L$$

$$\Rightarrow \Delta p = \frac{\tau_w * \pi d L}{d} \quad (20)$$

Equ (20) gives an expression for the pressure loss in a pipe in terms of the pipe diameter and the shear stress at the wall on the pipe. Hence, shear stress will vary with velocity of flow and hence with Re .

C. Pipeline Pressure Loss During Laminar Flow

For laminar flow, the pressure loss in a pipe is given by the Hagen Poiseuille Equation:

$$\Delta p = \frac{32 \mu L U}{d^2} \quad (21)$$

In terms of head,

$$H_f = \frac{32 \mu L U}{\rho g d^2}$$

Where $h_f = \text{head loss due to friction}$ and $\mu = \text{velocity}$.

D. Pipeline Pressure Loss During Turbulent Flow

Figure 5 shows a bounded fluid flow scenario flowing in a channel with $Re > 2000$, i.e. turbulent flow in both closed (pipes and ducts) and open (rivers and channels). In this case, consider the element of fluid shown in Figure 5 where the flow via the channel have length L and with perimeter P . The flow is steady and uniform, so that acceleration is zero and the flow area at sections L_1 and L_2 is equal to A .

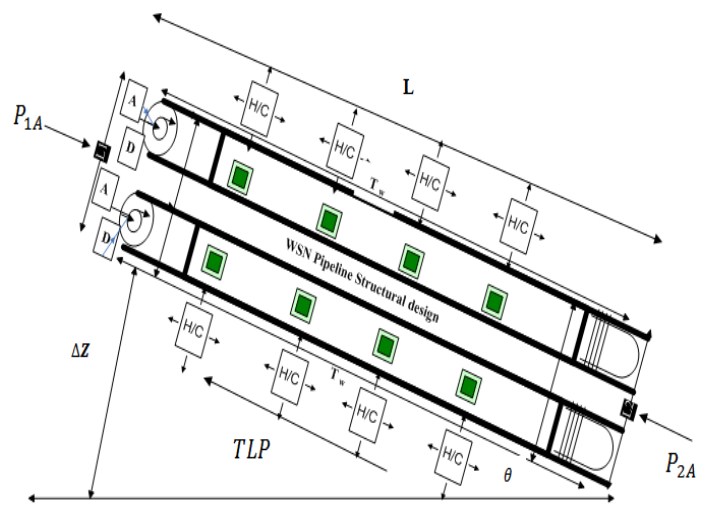


Fig. 5. Element of Fluid in a channel flowing with uniform flow.

From Figure 5,

$$P_1 A - P_2 A - \tau_w * LP + W \sin \theta = 0 \quad (22)$$

By arranging the weight term as $\rho g A l$ and $\sin \theta = -\Delta z / L$

$$A(P_1 - P_2) - \tau_w * LP - \rho g \Delta z = 0 \quad (23)$$

Hence,

$$\left[\frac{(P_1 - P_2) - \rho g \Delta z}{L} \right] - r_0 \frac{P}{A} = 0 \quad (24)$$

Where the first term represents the piezometric head-loss of the length L

$$r_0 = m \frac{dp}{dx} \quad (25)$$

Where $m = A/P$ is referred to as the hydraulic mean depth

By writing piezometric head loss as

$$P = \rho g h_f \quad (26)$$

Then, shear stress per unit length is given as

$$r_0 = m \frac{dp}{dx} = \frac{[m * \rho g h_f]}{L} \quad (27)$$

Equ (27) gives a relationship of shear stress at the wall to the wall of change in piezometric pressure.

But by introducing friction factor f given by

$$r_o = \frac{f \rho \mu^2}{2} \quad (28)$$

Where μ is the mean flow velocity,

$$\text{Hence, } \frac{dp}{dx} = \frac{f \rho \mu^2}{2m} = \frac{\rho g h f}{L} \quad (29)$$

So far, a general bound flow, head loss due to friction can be written as

$$hf = \frac{f L \mu^2}{2m} \quad (30)$$

More specifically, for a circular pipe,

$$m = A/P = \frac{\pi d^2}{4\pi d} = \frac{d}{4} \quad (31)$$

This then gives

$$hf = \frac{4f L \mu^2}{2gd} \quad (32)$$

Equ.(32) gives Darcy-Weisbach Equation for head loss in circular pipes. By rearranging Equ.(32) in terms of discharge Q using $Q = Au$, this implies that

$$U = \frac{4Q}{\pi d^2} \quad (33)$$

Substituting for U in Equ (32) gives

$$hf = \frac{64f L Q^2}{2g\pi^2 d^5} = \frac{f L Q^2}{3.03d^5} \quad (34)$$

$$\text{With 1\% Error } \rightarrow \frac{f L Q^2}{3d^5} \quad (35)$$

E. Pipeline Friction Factor

For laminar flow, there is a frictional constraint. From the foregoing, the Equ. derived for head loss in turbulent flow is equivalent to that derived for laminar flow with the difference being the empirical f . From Equ (34) and (35) Hagen Poiseuille and Darcy-weisbach equations give:

$$\frac{32\mu Lu}{\rho g d^2} = \frac{4f L u^2}{2gd} \quad (36)$$

Hence

$$f = \frac{16\mu}{\rho g v d} = \frac{16}{Re} \quad (37)$$

F. Pipeline Losses at Sudden Enlargement

Consider the flow in the sudden enlargement shown in the pipeline structure in Figure 6 with the fluid flow from section 1 to section 2. The velocity must reduce and so the pressure increases. The sensor nodes are placed as shown also. At position1, turbulent eddies occurs which give rise to the local head loss.

Applying the momentum equ. Between 1 and 2 gives,

$$P_1 A_1 - P_2 A_2 = P^* Q (U_2 - U_1) \quad (38)$$

Now, by using continuity equ. To remove Q i.e. (Substitute $Q = A_2 U_2$)

$$P_1 A_1 - P_2 A_2 = P A_2 U_2 (U_2 - U_1) \quad (39)$$

$$\text{Rearranging gives } \frac{P_2 - P_1}{P_g} = \frac{U_2}{g} (U_2 - U_1) \quad (40)$$

By applying the Bernoulli equ from point 1 to point 2 with the head loss term h_l

$$\frac{P_1}{P_g} + \frac{U_1^2}{2g} = \frac{P_2}{P_g} + \frac{U_2^2}{2g} + h_l \quad (41)$$

$$\text{By re-arranging gives } h_l = \frac{U_1^2 - U_2^2}{2g} - \frac{P_2 - P_1}{P_g} \quad (42)$$

By combining Equ 40 and 42, This gives

$$h_l = \frac{U_1^2 - U_2^2}{2g} - \frac{U_2}{g} (U_1 - U_2), \text{ this implies that} \quad (43)$$

$$h_l = \left(\frac{U_1^2 - U_2^2}{2g} \right)^2$$

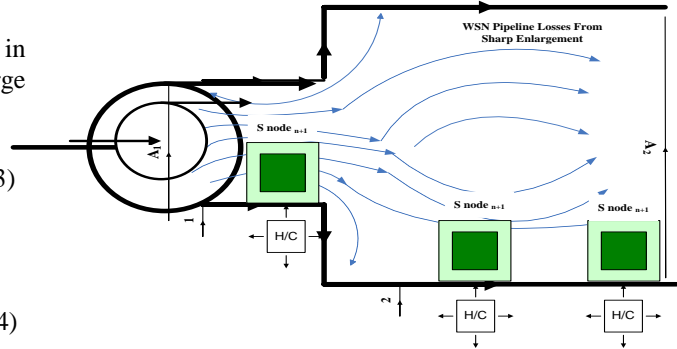


Fig. 6. WSN pipeline Sudden expansion model

Substituting again for the continuity equ. to get an expression involving the two areas i.e.,

$$Q_2 = U_1 A_1 / A_2, \text{ gives}$$

$$h_l = \left(1 - \frac{A_1}{A_2} \right)^2 \quad (44)$$

When a pipe expands into a large tank $A_1 \ll A_2 = 0$, so $K_l = 1$, i.e., the head loss = Velocity head just before the expansion into the tank.

G. Pipeline Energy Analysis for Flow Monitoring

Using Bernoulli Equ. which is a statement of conversion of energy along a streamline. By this principle, the total energy in the system does not change; hence the total head does not change. So the Bernoulli Equ can be written as

$$\frac{P}{P_g} + \frac{U^2}{2g} + Z = H = \text{Constant} \quad (45)$$

i.e. Total energy per unit weight = \sum (Pressure Energy Per Unit Weight + Kinetic Energy per Unit Weight + Potential Energy Per Unit Weight)

Where pressure head = $\frac{P}{P_g}$

Velocity head = $\frac{U^2}{2g}$

Potential head = Z

Total head = H

From Equ. (45), Bernoulli equation has some restrictions in its applications viz:

- i. Flow is Steady
- ii. Density is Constant i.e. fluid is incompressible
- iii. Frictional losses are negligible.

H. Pipeline Even Location Model

The CF-WAN based architecture proposed for SHM in pipeline systems seeks to monitor, maintain and protect gas, oil and water pipeline infrastructures. The design seeks to detect, locate and report anomalies such as leakages, corrosion, fracture and any other damages on the pipeline infrastructure. The system largely depend on network availability to be able to transfer the information gathered and report leakages or any other sensed data to the control station.

The connectivity of the network, the continuity of power supply, and the maintainability of the network are areas of concern in this research. Through the identification of pipe flow rate, pressure and temperature anomalies, the IoT WSN can then detect and localize leakages of small entity based on the distance map. Furthermore, the ability to pinpoint the exact location of the leak allows an immediate reaction at the event location, minimizing downtime and ecological consequences.

Figure 7 shows a typical architecture of pipeline sensors for event localization. In this case, locating an event on a pipeline requires the use of sensors on the opposite sides of the event. Using a pulse arriving times t_p and sensor position P_n , the location of an event such as vandalization, leakages along pipelines can be determined.

Consider Figure 7 showing a schematic pipeline with N key sensors denoted by S_1, S_2, S_3, S_4 at distances X_1, X_2, X_3, X_4 from the source. Assuming an impulse event occurs at some unknown location and the pulse generated is recorded by the sensors arriving at times t_1, t_2, t_3, t_4 , etc respectively, if the sensors are spaced at approximately equal intervals, the event will be located between the first two arrivals, between the 1 and 2.

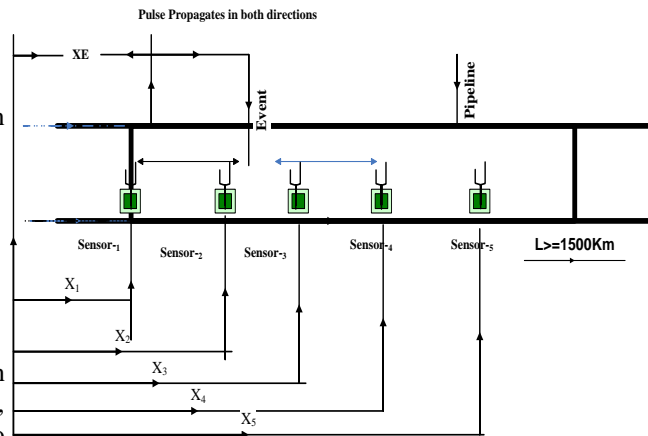


Fig. 7. Pipeline Sensors for event localization

The location of an event on the pipeline shown in Figure 7 can be determined with either sensor 2 or 3. The pulse propagation velocity C_p can be measured from the arrivals at the sensors on the same side of the event, Sensor 4 and 5.

The exact event location from sensor1, S_1 is given by

$$XE_1 = \sum_i^n \frac{(t_{12}C_p + X_{21})}{2} \quad (46)$$

or

From Sensor 2,

$$XE_2 = \sum_i^n \frac{(X_{21}C_p - C_p t_{12})}{2} \quad (47)$$

For sensor 3 and 4, considering the normal times as $t_{delay34}$, the velocity of propagation of the pressure pulse is given by

$$C_p = \frac{X_{3,4}}{t_{delay34}} \quad (48)$$

Where $X_{3,4}$ is the known distance between sensor 3 and 4

From these, any time the IoT WSN senses a leakage event, along the distance X_1 to X_{n+1} , it will quickly transmit it in a multi-hub fashion into the WAN Cloud as depicted in Figure 1.

V. CF-WAN IoT WIRELESS SENSOR NETWORK

A. Model Domain

Recall from Figure 1, the proposed CF-WAN IoT-WSN is an directed graph $G = \langle V, F \rangle$, where V represents the set of vertices and E represents the set of edges or links. The Sink interface is placed outside the area to be monitored. Let's assume that the IoT WSN consist of nodes linearly placed in a pipeline with an existing link $E(i,j)$ between the $node_i$ and $node_j$ with an Euclidean distance of $d(i,j)$ which must be less than the radio transmission radius R namely $d(i,j) < R$.

The unidirectional graph means directional communication link, i.e. if $node_j$ can receive packet from its neighbor or neighboring event, it will then transmit to the sink. The transmission of sensed data between S_1 and S_n requires a power from the battery model proportional to d_{ij} , where the d_{ij} , denotes the Euclidean distance between the source and sink.

Let

$$D = (\{p1, \dots, pk\}) \text{ be the set of pipes involved in a disaster vandalization.} \quad (49)$$

According to the mainstream disaster scenario, it is assumed that D also destroys all the sensors deployed on the affected pipes. However, it must be stressed that due to the data dispersal strategy used in the model, the sensed data produced by the eroded sensors are still available from the surviving sensors invasively deployed on the pipeline graph.

B. CF-WAN WSN Node Battery Model

The sensor nodes in Figure 1 depend on the battery model for effective data communication and life span sustainability within CF-WAN. This is developed in this section having carried out a survey on the main components of IoT WSN node viz: controller, radio modem, sensors/actuators, memory and batteries as shown in Figure 8. For the SHM architecture, this paper derived the relevant model for IoT WSN battery life and event location. Since the energy supply of mobile/sensor nodes is from the battery, the goal in Figure 8 is to provide as much energy as possible at smallest cost/volume/weight/recharge time/longevity.

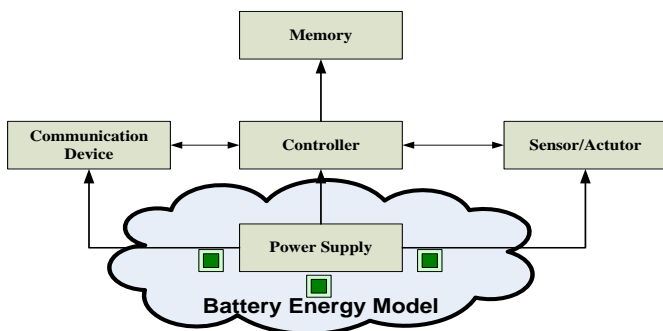


Fig 8: Energy Model of a WSN

The battery electrode in the battery connects with a dry electrolyte for energy harvesting. The requirements for both transmit and receive electronics include:

- Low self-discharge with low duty cycle
- Long shelf live
- Capacity under load
- Efficient discharging at low current
- Good relaxation properties (good self-discharging)
- Voltage stability

Figure 9 shows the battery model of the IoT WSN derived with the implemented energy parameters. It shows the model (CF-WAN WSN battery cell) using the Simscape language. This is used to achieve nonlinear equations of the equivalent circuit components. In this way, the connection between model components and the defining physical equations is more easily understood.

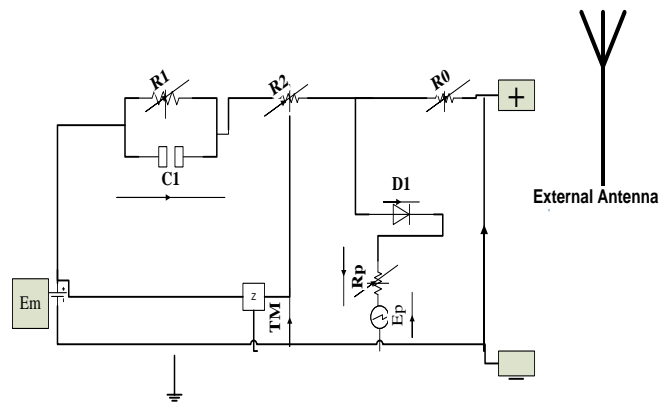


Fig. 9. Logical Model of the WSN battery

From Figure 9, the details of the battery model was carefully realized using the Simscape language for the nonlinear equations (i.e., equivalent circuit components), primarily via convection. The heating is primarily from battery internal resistance, $R2$.

The MATLAB was used to model the battery process model while observing the parametric variables as shown in the previous plots. In the MATLAB environment, Simscape electronics alongside with the source and sink blocks sets are used in data flow hierarchical modelling. The analysis of the dynamic battery model is based on the related energy equations previously discussed. Its primary interface is a blockset diagramming tool with its customizable set of block libraries in the environment. Using the MATLAB library which comes with built in battery and electric functions, the system was implemented with the plots shown in Figures 10 to Figure 15. These shows optimal results for edge node monitoring. The trade-off is the cost considerations for the IoT WSN nodes.

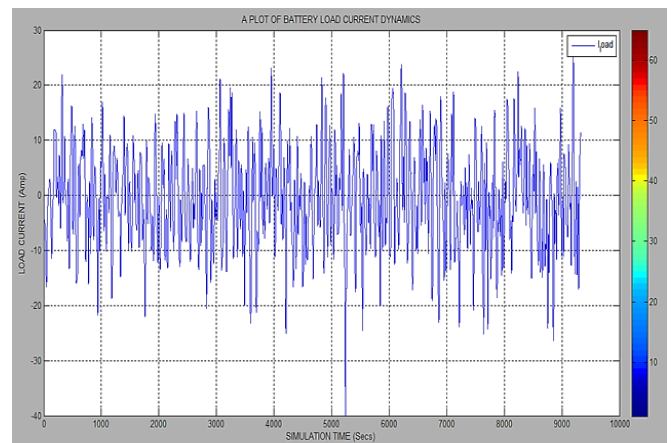


Fig. 10. A Plot battery load Current from the workspace

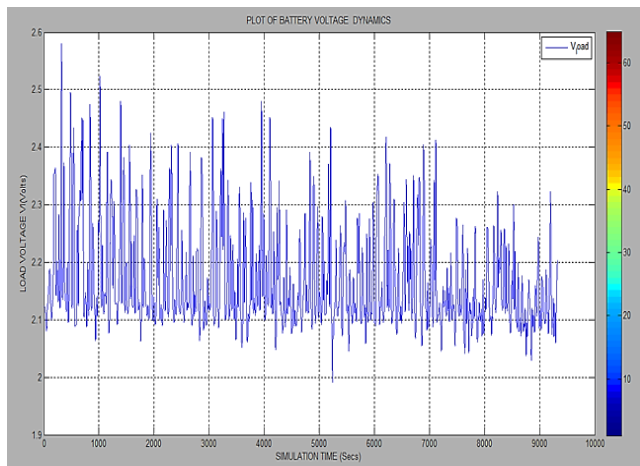


Fig. 11. WSN battery Voltage

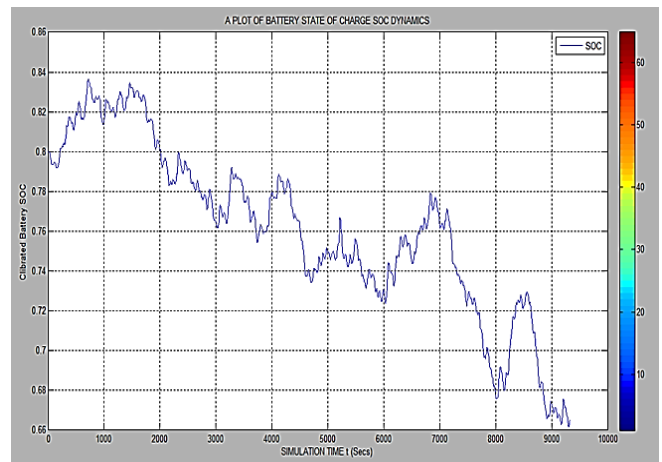


Fig. 13. WSN battery DOC.

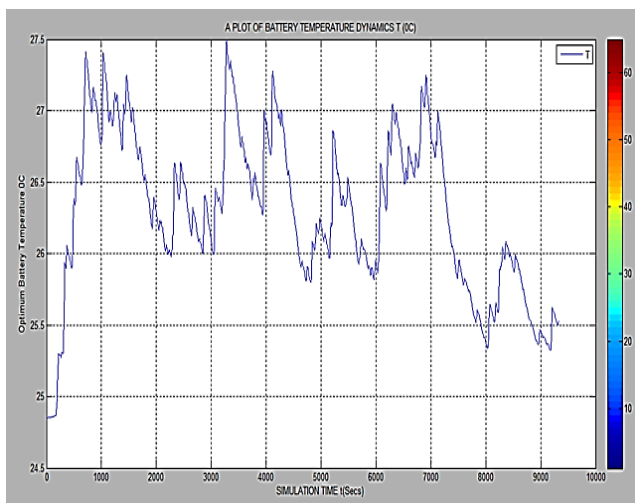


Fig. 12. A plot WSN battery Temperature °C

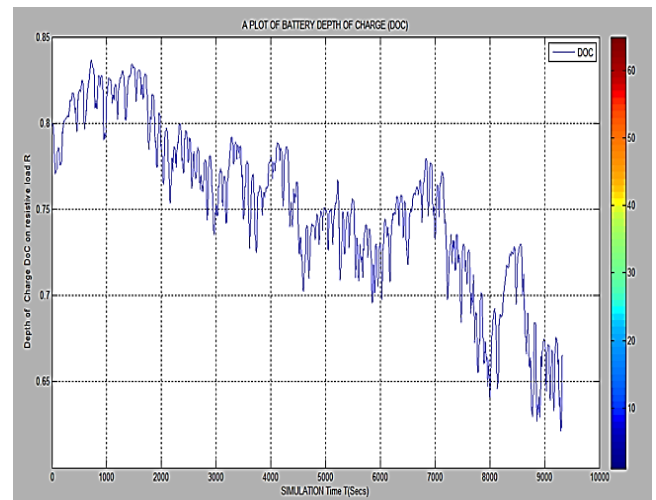


Fig. 14. WSN battery SOC.

Considering Figure 13 and 14, in battery taxonomy, Depth of Discharge (DOD) (%) is the percentage of battery capacity that has been discharged expressed as a percentage of maximum capacity as shown in Figure 13. A discharge to at least 80 % DOD is referred to as a deep discharge. Depth of discharge (DOD) is an alternate method to indicate a battery's state of charge (SOC).

The DOD is the complement of SOC: as one increases, the other decreases. While the SOC units are percent points (0% = empty; 100% = full), the units for DOD can be Ah (e.g., 0 = full, 50 Ah = empty) or percent points (100% = empty; 0% = full). As a battery may actually have higher capacity than its nominal rating, it is possible for the DOD value to exceed the full value (e.g.: 52 Ah or 110%), something that is not possible when using SOC.

Figure 15 shows the SoC giving an expression of the present battery capacity as a percentage of maximum capacity. In this case, SOC is calculated using current integration to determine the change in battery capacity over time.

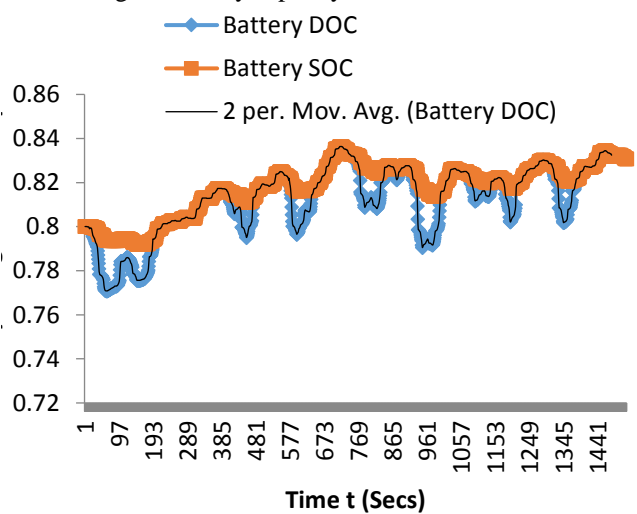


Fig. 15. Combined Charge Status/Combined Plot of Battery DoC Vs SoC.

VI. SYSTEM VALIDATION

Program Description Language (PDL) was used to script PROTEUS 7.6 ISIS while establishing the program algorithms. Protus ISIS 7.6 was used to develop a unified behavioral model of the WAN based Pipeline monitoring using the CF-WAN algorithm. The Algorithm I was used to generate the unified behaviour (Appendix I). Essentially, the algorithm defines the transactional processes involved in the CF-WAN framework for edge monitoring and signal transmission to the gateway considering a linear status and handshaking of the nodes with the gateways.

In the next section, a discussion on simulation validation outputs is presented. The oil pipeline IoT WSN sensors connects the linearly distributed network structure in Fig.16. The simulation parameters follows a typical oil pipeline flow model as depicted in Table 1 for both the battery model and the pipeline monitoring.

A. Simulation configuration

Protus ISIS is employed during the implementation of the traffic design attributes in Table 1. In designing the CF-WAN considering a use case oil pipeline model, the main goals are to maintain convergence report event based on location action points, and create a real time reporting of triggered events from the base WSN to the WAN sink for auditing and profiling. The unified simulation subsystem for the CF-WAN WSN monitoring is in two phases: the hardware subsystem at the remote WAN Sink and hardware subsystem at the pipeline network WSN end. Each of the subsystem is made up of the input, control and output interfaces whose parameters are detailed in Table 1.

Table 1: Simulation Traffic Attributes (Authors Field Dataset)

S/N	Parameters	Values
1	No of Pipeline hierarchies	3-A,B,C
2	Rate Constant	1700
3	Centrifugal Pumps	6
4	Reference Angular Velocity	1.77e+03 rpm
4	Oil Pipe Line Type/Number	Resistive Pipes LP/21
5	Distances	500Km-1500Km
6	Pipeline Cross Section Type	Circular
7	Internal Diameter	Station_1.Pipe_diameter (1mm)
8.	Geometric Shape factor	1m
9.	Internal Surface Roughness Height	0.005mm
10.	Laminar Flow Upper margin	2e+03
11.	Turbulent Flow Lower margin	4e+03
12.	Reference Density	1000kg/m ³
13.	Number of Sensor Nodes	17sensors
16	Solver for Metrics	1-Linear Algebra (Sparse)
17.	No of Resistive Pipes – LP	21

At the implementation phase, MKR 1000, microcontroller was deployed at the pipeline locations A, B and C, while logically connecting to the remote site-WAN sink. The Algorithm I was integrated while the output subsystem at the CF-WAN Sink remote site was enabled. This is made up the virtual terminal logically connected to the IoT WSN

controllers which displays the flow rate, pressure, temperature, etc on virtual terminal scope in real time . The output subsystem at the operator’s site (CF-WAN Sink) is a virtual graphical user interface (GUI) comprising LED indicators, LCD, buzzer and Central Server. Proteus Virtual Simulation Module (PVSM) was used to develop the output subsystem. The CF-WAN IoT WSN algorithm that runs on the sensor controllers is implemented using Algorithm I.

In this case, the central server (CF-WAN) receives that data sent from the remote IoT WSNs, interprets it and displays the information on the virtual LCD. The server also compares the received data with predefined thresholds and activates alarm when the events for vandalization occurs signifying the danger state. Figure 16 and 17 depicts the pipeline monitoring scenarios. Basically, Figure 17 illustrates CF-WAN IoT WSN system detection at sink showing vandalization on pipelines A, B and C.



Fig. 16: CF-WAN IoT WSN System Initialization

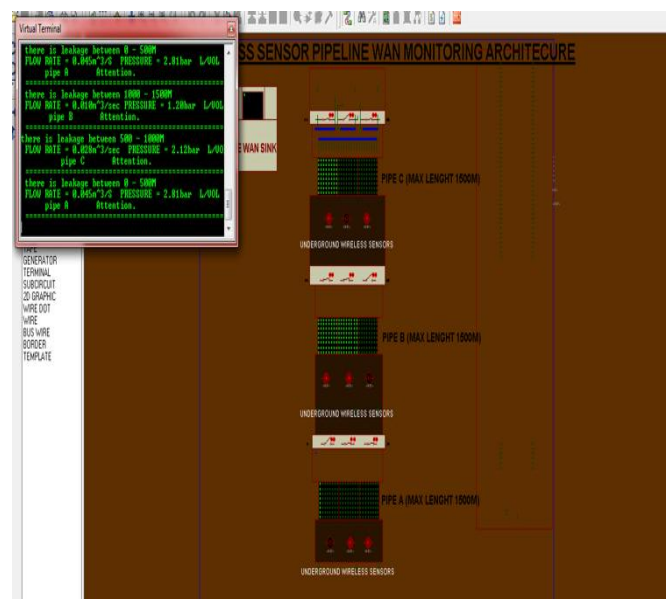


Fig. 17. CF-WAN System Detection at Sink showing Vandalization.

VII. CONCLUSION

In this paper, CF-WAN system for pipeline monitoring and leakage detection using IoT WSN is presented. The proposed solution highlights a new proof of concept for fluid monitoring and leakage detection. A framework for structural pipeline monitoring is targeted at existing pipeline facilities. The performance on a real world pipeline monitoring system will satisfy the metrics of good energy conservation on the battery model, robust pipeline design, and communication deployment. During the simulation, the data were captured via the Simevent "To Workspace block" for the battery model. This send inputs signal and writes the signal data to the MATLAB workspace. The work showed how MATLAB block writes the data to an array structure allowing for battery plots. Data were generated for remote analysis. In the work, remote network based facility was used to obtain flexible monitoring with precision at various distances. The pipeline model, the battery model and the unified model were shown to yield satisfactory results. This can be applied in oil and water managing scenario. Future work will detail other practical application context for CF-WAN applications. The use of machine learning algorithms for pipeline monitoring and remote analytics will be considered in future studies.

REFERENCES

- [1.] D. Liaw, Y. Hsieh, J. Lai and C. Chiu, "A network topology design for structural health monitoring," 2011 8th *Asian Control Conference (ASCC)*, Kaohsiung, 2011, pp. 665-670.
- [2.] C. Scuro, P. F. Sciammarella, F. Lamonaca, R. S. Olivito and D. L. Carni, "IoT for structural health monitoring," in *IEEE Instrumentation & Measurement Magazine*, vol. 21, no. 6, pp. 4-14, December 2018, doi: 10.1109/MIM.2018.8573586.
- [3.] T. Jirsik and P. Celeda, "Cyber Situation Awareness via IP Flow Monitoring," NOMS 2020 - 2020 *IEEE/IFIP Network Operations and Management Symposium*, Budapest, Hungary, 2020, pp. 1-6, doi: 10.1109/NOMS47738.2020.9110327.
- [4.] M. Elleuchi, R. Khelif, M. Kharrat, M. Aseeri, A. Obeid and M. Abid, "Water Pipeline Monitoring and Leak Detection using soil moisture Sensors: IoT based solution," 2019 16th *International Multi-Conference on Systems, Signals & Devices (SSD)*, Istanbul, Turkey, 2019, pp. 772-775, doi: 10.1109/SSD.2019.8893200.
- [5.] K. C. Okafor, G.C. Ononiwu, Sam G. V.C Chijindu, C. C. Udeze "Towards Complex Dynamic Fog Network Orchestration Using Embedded Neural Switch", In *International Journal of Computers and Applications, (IJCA) SI- Internet of Everything, Networks, Application, and Computing Systems*. United Kingdom. Print ISSN: 1206-212X Online ISSN: 1925-7074. 2018, Vol.40 (4), Pp.1-18.
- [6.] K.C. Okafor, I.E Achumba, G.A Chukwudebe, G.C Ononiwu, "Leveraging Fog Computing For Scalable IoT Datacenter Using Spine-Leaf Network Topology", *Journal of Electrical and Computer Engineering*, Vol.2017, Article ID 2363240, Pp.1-11.
- [7.] Yanxiang Jiang; Chaoyi Wan; Meixia Tao; Fu-Chun Zheng; Pengcheng Zhu; Xiqi Gao; Xiaohu You, "Analysis and Optimization of Fog Radio Access Networks with Hybrid Caching: Delay and Energy Efficiency," in *IEEE Transactions on Wireless Communications*, doi: 10.1109/TWC.2020.3023094.
- [8.] S. Mishra, M. N. Sahoo, S. Bakshi and J. J. P. C. Rodrigues, "Dynamic Resource Allocation in Fog-Cloud Hybrid Systems Using Multicriteria AHP Techniques," in *IEEE Internet of Things Journal*, vol. 7, no. 9, pp. 8993-9000, Sept. 2020, doi: 10.1109/JIOT.2020.3001603.
- [9.] Y. Jiang et al., "Analysis and Optimization of Cache-Enabled Fog Radio Access Networks: Successful Transmission Probability, Fractional Offloaded Traffic and Delay," in *IEEE Transactions on Vehicular Technology*, vol. 69, no. 5, pp. 5219-5231, May 2020, doi: 10.1109/TVT.2020.2981122.
- [10.] C. Swain et al., "METO: Matching Theory Based Efficient Task Offloading in IoT-Fog Interconnection Networks," in *IEEE Internet of Things Journal*, doi: 10.1109/JIOT.2020.3025631.
- [11.] A. Kara, M. A. Al Imran and K. Karadag, "Linear Wireless Sensor Networks for Cathodic Protection Monitoring of Pipelines," 2019 International Conference on Mechatronics, Robotics and Systems Engineering (MoRSE), Bali, Indonesia, 2019, pp. 233-236, doi: 10.1109/MoRSE48060.2019.8998664.
- [12.] B. Han and Q. Fu, "Study on Fiber Bragg Grating Monitoring Technology for Oil and Gas Pipelines Crossing the Landslide," 2019 *IEEE 11th International Conference on Communication Software and Networks (ICCSN)*, Chongqing, China, 2019, pp. 57-61, doi: 10.1109/ICCSN.2019.8905306.
- [13.] L. Qiu, Z. Salcic and K. I. Wang, "Adaptive Duty Cycle MAC Protocol of Low Energy WSN for Monitoring Underground Pipelines," 2019 *IEEE 17th International Conference on Industrial Informatics (INDIN)*, Helsinki, Finland, 2019, pp. 41-44, doi: 10.1109/INDIN41052.2019.8972234.
- [14.] S. Razvarz, C. Vargas-Jarillo and R. Jafari, "Pipeline Monitoring Architecture Based on Observability and Controllability Analysis," 2019 *IEEE International Conference on Mechatronics (ICM)*, Ilmenau, Germany, 2019, pp. 420-423, doi: 10.1109/ICMECH.2019.8722875.
- [15.] J. M. Coronado, A. Badillo-Olvera and O. Begovich, "A Wireless Low-Cost Monitoring System for Leak Diagnosis in Water Transmission Pipelines Based on Arduino-Xbee Technology," 2019 *IEEE International Autumn Meeting on Power, Electronics and Computing (ROPEC)*, Ixtapa, Mexico, 2019, pp. 1-6, doi: 10.1109/ROPEC48299.2019.9057076.
- [16.] M. Guan, Y. Cheng, Q. Li, C. Wang, X. Fang and J. Yu, "An Effective Method for Submarine Buried Pipeline Detection via Multi-Sensor Data Fusion," in *IEEE Access*, vol. 7, pp. 125300-125309, 2019, doi: 10.1109/ACCESS.2019.2938264.
- [17.] R. J. Cintra, T. V. de Oliveira and M. P. Mintchev, "Wireless Network for Real-Time Detection of Pipeline Leakages," 2019 Big Data, *Knowledge and Control Systems Engineering (BdKCSE)*, Sofia, Bulgaria, 2019, pp. 1-5, doi: 10.1109/BdKCSE48644.2019.9010605.
- [18.] M. A. Uddin, M. Mohibul hossain, A. Ahmed, H. H. Sabuj and S. Yasar Seaum, "Leakage Detection in Water Pipeline Using Micro-controller," 2019 1st *International Conference on Advances in Science, Engineering and Robotics Technology (ICASERT)*, Dhaka, Bangladesh, 2019, pp. 1-4, doi: 10.1109/ICASERT.2019.8934648.
- [19.] S. Sapre and J. P. Shinde, "Water Pipeline Monitoring on Cloud & Leakage Detection with a Portable Device," 2019 *IEEE Pune Section International Conference (PuneCon)*, Pune, India, 2019, pp. 1-5, doi: 10.1109/PuneCon46936.2019.9105760.
- [20.] M. Ren, X. Chen and H. Yu, "Real-time monitoring method of pipeline deformation based on Internet of things," 2019 2nd *International Conference on Safety Produce Informatization (IICSPI)*, Chongqing, China, 2019, pp. 114-118, doi: 10.1109/IICSPI48186.2019.9096033.
- [21.] N. Ahmed, Q. Gang, A. Ahmad, D. Ali, M. Muzzammil and S. Liu, "Oil and Gas Pipeline Monitoring Through Magneto-Coupled Wireless Sensor Network," *OCEANS 2019 - Marseille*, Marseille, France, 2019, pp. 1-4, doi: 10.1109/OCEANSE.2019.8867200.
- [22.] A. B. Yazid, J. Chijioke, M. B. Mahamat, H. I. Ahmad, V. C. Anye and M. Zakariya, "Real-time Pipeline Vandalism Detection Using Open-Circuit Technique," 2019 15th *International*

- Conference on Electronics, Computer and Computation (ICECCO)*, Abuja, Nigeria, 2019, pp. 1-4, doi: 10.1109/ICECCO48375.2019.9043222.
- [23.] N. Mangayarkarasi, G. Raghuraman and S. Kavitha, "Influence of Computer Vision and IoT for Pipeline Inspection-A Review," 2019 *International Conference on Computational Intelligence in Data Science (ICCIDS)*, Chennai, India, 2019, pp. 1-6, doi: 10.1109/ICCIDS.2019.8862109.
- [24.] X. Liu and H. Wang, "Study on the Construction of VIV Monitoring Information System for the Free Spanning," 2019 *IEEE 5th International Conference on Computer and Communications (ICCC)*, Chengdu, China, 2019, pp. 1393-1397, doi: 10.1109/ICCC47050.2019.9064304.
- [25.] A. Abrardo, A. Fort, E. Landi, M. Mugnaini, E. Panzardi and A. Pozzebon, "Black Powder Flow Monitoring in Pipelines by Means of Multi-Hop LoRa Networks," 2019 *II Workshop on Metrology for Industry 4.0 and IoT (MetroInd4.0&IoT)*, Naples, Italy, 2019, pp. 312-316, doi: 10.1109/METROI4.2019.8792890.
- [26.] R. Dzhalala, V. Dzhalala, B. Horon, O. Senyuk and B. Verbenets', "Information Technology of Surveys and Diagnostics of Underground Pipelines," 2019 *XIth International Scientific and Practical Conference on Electronics and Information Technologies (ELIT)*, Lviv, Ukraine, 2019, pp. 214-217, doi: 10.1109/ELIT.2019.8892295.
- [27.] O. N. Kuzyakov, M. A. Andreeva and I. N. Gluhih, "Corrosion Monitoring System for Field Pipeline Applying CBR Method," 2019 *International Multi-Conference on Industrial Engineering and Modern Technologies (FarEastCon)*, Vladivostok, Russia, 2019, pp. 1-6, doi: 10.1109/FarEastCon.2019.8934396.
- [28.] V. Sudevan, A. Shukla and H. Karki, "Hierarchical Controller for Autonomous Tracking of Buried Oil and Gas Pipelines and Geotagging of Buried Pipeline Structure," 2019 *IEEE International Conference on Cybernetics and Intelligent Systems (CIS) and IEEE Conference on Robotics, Automation and Mechatronics (RAM)*, Bangkok, Thailand, 2019, pp. 338-343, doi: 10.1109/CIS-RAM47153.2019.9095799.
- [29.] N. K. A. Thabet, V. Fetisov and O. Dmitriyev, "Electric Heating Unit for Oil Pipeline Paraffin Deposit Monitoring System," 2019 *International Conference on Electrotechnical Complexes and Systems (ICOECS)*, Ufa, Russia, 2019, pp. 1-4, doi: 10.1109/ICOECS46375.2019.8949943.
- [30.] K. Ma and H. Leung, "Sparse spatiotemporal feature learning for pipeline anomaly detection," 2019 *IEEE 18th International Conference on Cognitive Informatics & Cognitive Computing (ICCI*CC)*, Milan, Italy, 2019, pp. 123-129, doi: 10.1109/ICCICC46617.2019.9146048.
- [31.] M. Abdelhafidh, M. Fourati, L. C. Fourati, A. ben Mnaouer and M. Zid, "Novel Data Pre-processing Algorithm for WSN Lifetime Maximization in Water Pipeline Monitoring System," 2019 *IEEE Wireless Communications and Networking Conference (WCNC)*, Marrakesh, Morocco, 2019, pp. 1-6, doi: 10.1109/WCNC.2019.8885808.
- [32.] H. Jiang, J. Gao, F. Xia, X. Zhang, T. Zhou and D. Liu, "Fault Recognition Technology for Pipeline Systems Based on Multi-feature Fusion of Monitoring Data," 2019 *IEEE International Conference on Prognostics and Health Management (ICPHM)*, San Francisco, CA, USA, 2019, pp. 1-7, doi: 10.1109/ICPHM.2019.8819415.

Appendix I:

Algorithm I: WAN WSN Transmission Algorithm {SHM}

Begin ()

Fog_Container

Aggregation History of Edge IoT WSN

CF_WAN_monitorCall_edge_Schedule
QoS parameterStatus // Latency, Throughput & Service availability
 CF_WAN_decision ← Empty;
 Cloud_excessVM ← Empty;

For $S_n = 1$ to $N(j)$

// CF_WAN_Monitor

Recycle every (1sec)_CF_WAN_monitorCallPeriod minutes

// Analyzer

Procedure () Wait for predefined period and store any Ready information received during this period

Procedure () Calculate the leakage event for each ready message information that is to be stored in the node

MAC table

Procedure () Send Engagement to the WAN gateway with the best transmit energy.

If (Engagement Acceptance is received) **Then** open gateway &&
 Calculate the Sensor node ID))

Return

If (sensor node is in fixed linear status) **Then** check if (targets event have been sensed)

If (next node exists around the targets) **Then** check if (node clock ready)

If (Clock ready Ok) **Then** frames as Packets

ELSE locate the next node and check its radius/position; check the buffer content;

Else check all the MAC layer parameters && get ready for a Direct multihop flow

End If

Else Continue to move with linear angle

Else If (sensor is in active status)

Then Recording: receiving data; change status; processing, checking pipeline & waiting time; select next node to sink; send update via the node to sink;

Else Recording: keep tracking the linear path

Keep forwarding Ack to WAN Sink

End if

End If

end return
